Light Metals 2014
Edited by: John Grandfield
TMS (The Minerals, Metals & Materials Society), 2014

Electromagnetic Stirring in Melting Furnaces - a Critical Evaluation

Andreas Buchholz, Georg Rombach, Gerd-Ulrich Gruen
Hydro Aluminium Rolled Products GmbH, Research & Development; Georg-von-Boeselager-St. 21; 53117 Bonn, Germany

Keywords: electro-magnetic stirring, numerical simulation, energy efficiency

Abstract

Although electromagnetic stirring has been in industrial use in the aluminium industry since the sixties of the 20th century, it has faced a revival in recent years under the pressure of increasing energy prices, challenges to raise production in existing installations and the appearance of innovative and competing stirrer systems in the market. The usually claimed benefits vary between 5 and 20 percent reduction in energy consumption, cycle time and dross generation. The authors will present an overview of their efforts to develop a modeling toolset to analyze the advantages of the different technologies and will describe the difficulties to develop an objective picture to monitor the improvements in real installations. The future challenges in modeling will be discussed and recommendations will be given for a better comparison of the performance of the different systems.

Introduction

The typical heating in a reverberatory furnace is from top to bottom. The burner flames heat the melt partially directly by convection and conduction but mainly indirectly by radiation of the roof. As soon as liquid melt exists, the stratification of the liquid leads to the formation of a rather stable temperature gradient (Fig. 1). Typically these gradients are in the order of 1-2 K/cm. Due to the stratification the convection inside the melt is damped and the heat transfer is dominated by conduction. The hot surface layer increases the re-radiation and limits the heat pickup from roof and furnace gases. The basic idea behind melt stirring is to increase the heat transfer inside the melt by an imposed strong motion. This will reduce the thermal gradients inside the melt and lower the temperature at the surface. Since the temperature difference between melt surface and furnace atmosphere becomes larger, it is expected that more energy is extracted from the radiation space.

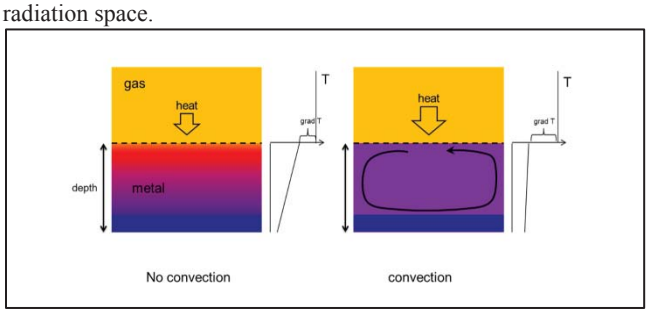

Fig. 1: Basic impact of stirring

An elegant way to introduce a forced motion is to apply electromagnetic stirring, since a mechanical contact between stirrer device and melt can be avoided completely. In the most basic setup a rotating permanent magnet is sufficient to generate the desired effect: The magnetic field penetrates furnace walls and metal. Due the local change of magnetic field eddy currents are induced in the metal according to Faraday's law. The induced currents couple with the magnetic field to generate a propelling Lorentz-force, which causes the fluid motion (Fig. 2). A similar effect can be achieved by a sequence of six coils fed with the three phases of rotary currents. By choosing an appropriate order the current in each coil is shifted by 60 ° from the previous. The superposed magnetic fields of all coils are imitating the field of the rotating permanent magnet.

All technically available electromagnetic stirrers can be considered as variations of these two basic setups. These are mainly axial magnetic pumps, bottom stirrers and permanent magnet stirrers. The specific differences follow from the pole distances, the magnitude of electric currents or the magnetization of permanent magnet material and the applied frequency or rotational speed, which decide how far the magnetic field and the force field may penetrate into the metal. The industrial utilization started in the steel industry in the 1950s [1] and a decade later in aluminium industry.

So far the basic mechanisms appear to be comprehensive, but when trying to get quantitative figures about the benefits of stirring it is difficult to get consistent information. Furthermore, performing reliable measurements under practical conditions is less straightforward than appears at first glance, as will be discussed later on. These problems gave rise to look into electro-magnetic stirring from a more theoretical basis. An existing numerical model of reverberatory furnace [2] appeared to be a promising platform to include electromagnetic stirring mechanisms. In the following this model approach and some of the applications will be presented and the conclusions discussed.

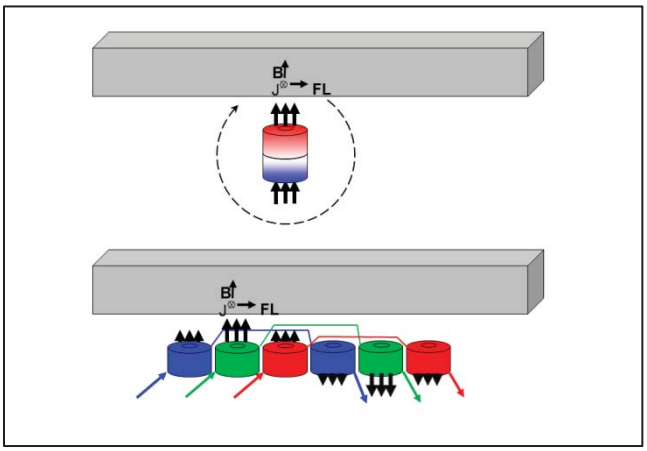

Fig. 2: Basic mechanisms of electromagnetic stirring: Rotating permanent magnet and coil arrangement fed with 3 phases of rotary currents imitating rotating permanent magnet.

Modeling approach

Basic model

The original modeling approach is based on the CFD (computational fluid dynamics) software ANSYS Fluent 14.0, the ANSYS Fluent MHD module and the electro-magnetics software package ANSYS Maxwell 15.0. The further explanations will focus on the electromagnetic problem, since heat and flow calculations are more common and already presented elsewhere [2].

ANSYS Maxwell calculates a so-called "external" magnetic field B_0 generated by a coil arrangement and imposed electric currents with or without the presence of additional conducting material. The Fluent MHD module utilizes this external field to calculate a modified B field, which includes the impact of local flow velocity. The MHD module is capable process external fields, which were computed with or without a metal charge. It turned out that the former approach provides faster convergence in the Fluent calculations, and this became the standard method to calculate the external magnetic field, i.e. the metal charge is already present in the calculation of the external field, but the velocities are fixed to zero.

Both ANSYS Maxwell and MHD model solve an induction equation for the B-field [3]:

$$\frac{\partial \vec{B}}{\partial t}+(\vec{v}\cdot\nabla)\vec{B}=\frac{1}{\mu\sigma}\nabla^2\vec{B}+(\vec{B}\cdot\nabla)\vec{v} \quad (1)$$

which can be derived from Maxwell's equations assuming no free charges and slowly varying fields (compared to velocity of light) and Ohm's law for current density

$$\vec{J}=\sigma(\vec{E}+\vec{v}\times\vec{B}) \quad (2)$$

Since in the ANSYS Maxwell calculation the flow velocity is assumed to be zero, the calculation of the external magnetic field can be simplified:

$$\frac{\partial \vec{B}_0}{\partial t}=\frac{1}{\mu\sigma}\nabla^2\vec{B}_0 \quad (3)$$

The modified B field can be described as a superposition of the external field B_0 and the disturbances b caused by the impact of flow velocity

$$\vec{B}=\vec{B}_0+\vec{b} \quad (4)$$

Inserting (4) and (3) into (1) gives the induction equation for magnetic field disturbance b:

$$\frac{\partial \vec{b}}{\partial t}+(\vec{v}\cdot\nabla)\vec{b}=\frac{1}{\mu\sigma}\nabla^2\vec{b}+\left((\vec{B}_0+\vec{b})\cdot\nabla\right)\vec{v}-(\vec{v}\cdot\nabla)\vec{B}_0 \quad (5)$$

This equation is actually solved in the Fluent MHD module. The total B-field is calculated according to (4), which is then utilized to calculate the current density

$$\vec{J}=\frac{1}{\mu}\nabla\times\vec{B} \quad (6)$$

and the Lorentz-forces

$$\vec{F}_L=\vec{J}\times\vec{B} \quad (7)$$

which are incorporated as source terms in the Fluent momentum equations.

The actual coupling between ANSYS Maxwell and Fluent MHD module is a one way import of a so called harmonic solution of (1), i.e. the solution is split into a space dependent complex amplitude and a time-dependent factor

$$B_0(x,y,z,t)=\hat{B}_0(x,y,z)e^{i(\omega t+\varphi)} \quad (8)$$

The advantage of this method is that only a snapshot of the magnetic field (real and imaginary part) and its frequency are needed to describe the whole evolution in time.

Extensions

A big disadvantage of the basic approach is its limitation to fully transient calculations in Fluent. When calculating an axial electromagnetic pump, which is frequently run with grid frequency (50 Hz), the time step size is typically in the order of milliseconds. To calculate from zero velocities to a stationary state some thousand time steps are needed in Fluent, which can take several hours even on a 2d axi-symmetric case.

To speed up the calculations a simplified approach was introduced (see Fig. 4). The Lorentz-forces were calculated for zero velocities directly in ANSYS Maxwell and time averaged force components were derived using the following formulas (in Cartesian coordinates):

$$\langle FL_x\rangle=\frac{1}{2}\left[|\hat{J}_y||\hat{B}_z|\cos\left(\measuredangle(\hat{J}_y,\hat{B}_z)\right)-|\hat{J}_z||\hat{B}_y|\cos\left(\measuredangle(\hat{J}_z,\hat{B}_y)\right)\right]$$
$$\langle FL_y\rangle=\frac{1}{2}\left[|\hat{J}_z||\hat{B}_x|\cos\left(\measuredangle(\hat{J}_z,\hat{B}_x)\right)-|\hat{J}_x||\hat{B}_z|\cos\left(\measuredangle(\hat{J}_x,\hat{B}_z)\right)\right]$$
$$\langle FL_z\rangle=\frac{1}{2}\left[|\hat{J}_x||\hat{B}_y|\cos\left(\measuredangle(\hat{J}_x,\hat{B}_y)\right)-|\hat{J}_y||\hat{B}_x|\cos\left(\measuredangle(\hat{J}_y,\hat{B}_x)\right)\right] \quad (9)$$

In these equations $\langle\ldots\rangle$ denotes a time averaged value, $|\hat{\ldots}|$ the magnitude of a complex quantity and $\measuredangle(\hat{\ldots},\hat{\ldots})$ the phase angle between two complex quantities. The implementation in Maxwell is performed by a calculation tool in the postprocessor.

The time averaged Lorentz forces are imported directly into a Fluent flow calculation without utilization of the MHD module. This force term can be applied even in a stationary analysis. Although the simplification neglects the modification of the magnetic field by the developing flow, it turned out that the achieved results are still reasonably close to the fully transient computation with the MHD module. In the calculation of an axial electro-magnetic pump the throughput of the stationary approach differed from the transient solution by less than 15%, which appears to be an acceptable value since the calculation was sped up by a factor of 20.

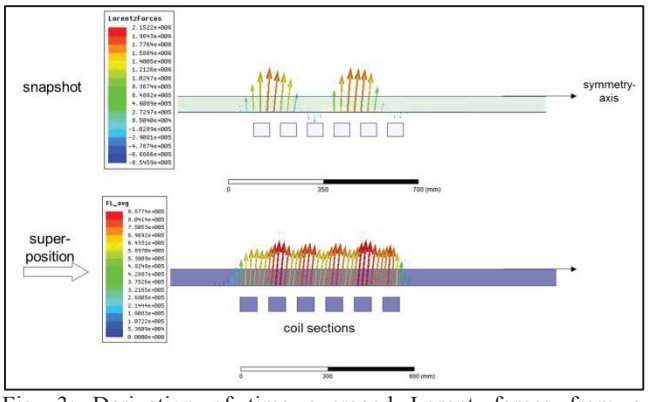

Fig. 3: Derivation of time averaged Lorentz-forces from a transient solution of force field in a transient 2d-axisysmmetric analysis of an electromagnetic pump.

The concept of the time-averaged Lorentz-force can be easily extended to configurations with rotating permanent magnets (Fig. 4). ANSYS Maxwell offers this capability by using automatic mesh adaptation in a fully transient calculation. The transient magnetic field generated in these calculations is not

compatible with the Fluent MHD module, which requires a harmonic solution (8) of the B-field as input. The direct import of time averaged Lorentz forces is more straightforward. The typical workflow of such an analysis is:

1. Perform a transient analysis in ANSYS Maxwell until forces or torques get stationary or periodic.
2. Calculate the arithmetic averages of the local Lorentz forces from all time steps of the last rotation period.
3. Export the time-averaged Lorentz force field into Fluent by customized subroutines.

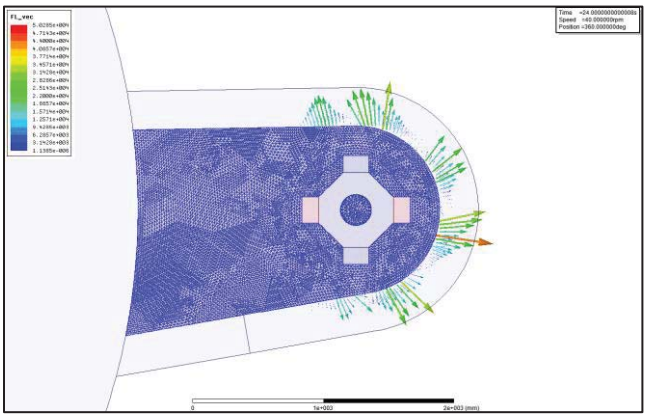

Fig. 4: Modeling rotating magnets using an adaptive mesh approach in ANSYS Maxwell.

It is even possible to derive a "pseudo-harmonic" solution, which can be used as input for the Fluent module. As before, the transient analysis is conducted again until stationary or periodic torques are achieved. Then the B-field values B(x,y,z,t) of the N time steps of one period are recorded and the discrete Fourier integrals are calculated to get the first Fourier coefficients:

$$B_{real}(x,y,z) = \frac{2}{N}\sum_{i=1}^{N} \sin(\omega t_i)\, B(t_i)$$
$$B_{imag}(x,y,z) = \frac{2}{N}\sum_{i=1}^{N} \cos(\omega t_i)\, B(t_i) \qquad (10)$$

These values, together with the frequency of the field provide the required input for the Fluent MHD module to perform a transient analysis.

Altogether, the present modeling toolbox offers capabilities to model the following setups (Fig. 5):

1. fully transient for coil system and AC currents,
2. time averaged force field for coil system and AC currents,
3. time averaged force field for rotating magnet stirrer,
4. transient model of permanent stirrer using a pseudo-harmonic magnetic field solution of rotating magnets.

One limitation of the one way coupling is that the change of electrical conductivity during melting is not considered in the present model. For aluminium the change of electrical conductivity from room temperature to fully liquid is considerable. The liquid value is only about 1/10 of the room temperature value [4], and still for the transition at the melting point the reduction is a factor of 2.2 [5]. Since the conductivity enters the formula of penetration depth of the magnetic field by $= \frac{1}{\sqrt{\pi\mu\sigma f}}$, this means that for a stirrer frequency of 0.7 Hz the penetration depth is only 10 cm, just below liquidus 20 cm and just above 30 cm. This can have a severe impact on the onset of a stirring effect during a melting process. For the time being this has to be mitigated by an appropriate choice of the conductivity of the more relevant state (liquid or solid).

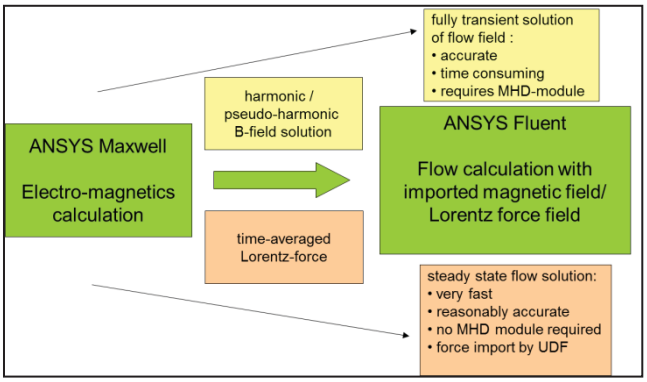

Fig. 5: Overview of coupling schemes of electromagnetics code ANSYS Maxwell and CFD code ANSYS Fluent.

Validation of models

To gain confidence in the reliability of the results in the beginning mainly consistency checks were performed using different model options. Furthermore, the impact of mesh refining in rather simple setups of axial electromagnetic pumps was investigated and compared with supplier data, which gave reasonable agreement concerning throughput values. In these calculations it turned out that the major force component of the Lorentz forces is directed towards the pump axis and only a smaller part generates a propelling effect (Fig. 3). This can explain the clogging effect, which is observed sometimes in this type of pumps (Fig. 6): Non-conducting particles face an opposite reaction force, which is 75% of the force on the equivalent amount of displaced melt [6].

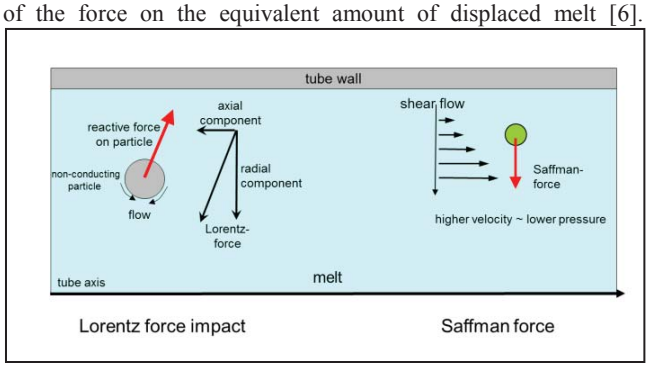

Fig. 6: Force field and clogging effect in EM pump tube due to reaction forces on non-conducting particles

In combination with a discrete particle model this effect can be even studied in the model quantitatively (Fig.7).
One supplier gave access to conduct B field measurements on top of a bottom stirrer and provided some details of the coil arrangement. It turned out that with a rather coarse setup the measured B-field could be reconstructed with the model (Fig. 8).
Although suppliers of electromagnetic devices usually are reluctant to reveal internal details, some important information can be gained by rather simple observations in operating plants. Magnetic dust particles usually leave characteristic footprints on the stainless steel window underneath a furnace revealing details of the pole arrangement (Fig. 9). Together with the external stirrer dimensions, power rating and frequency this information can be used to set up an initial model of a stirrer.

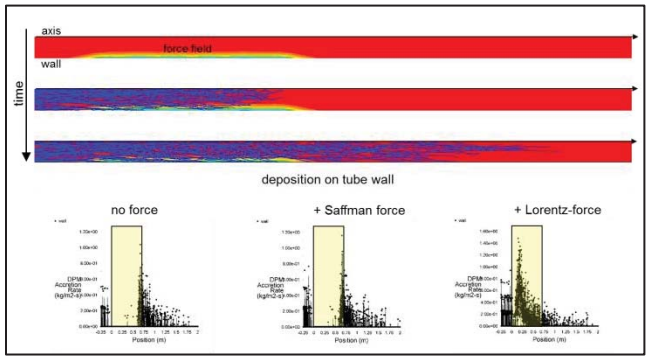

Fig. 7: Congestion of particles due to electromagnetic forces in an axial pump.

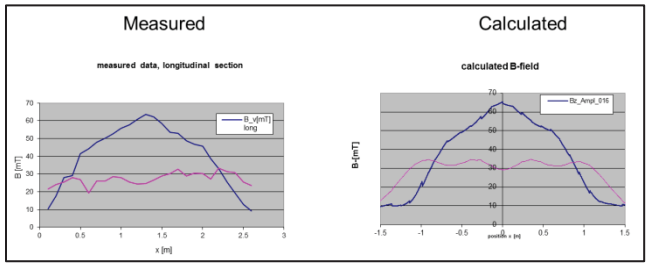

Fig. 8: Validation of magnetic field calculations: Measured vertical B-field components versus calculated values.

Fig. 9: Pole marks on stainless steel window reveal details of internal stirrer structure.

Application of model

The model found a major application in a study of potential performance increase of a remelting furnace by electro-magnetic stirring. This furnace has a capacity of 30 – 45 mt, a rather shallow bath depth of 30 to 45 cm and a melting rate of 9-15 mt/h. For this purpose the time averaged Lorentz force approach was combined with a melting model, which is an extended version of the model described earlier [2], accounting for latent heat and the advective transport of latent heat in the liquid. This melting model resembles the built-in solidification model of Fluent, but can be combined with combustion chemistry. The solid fraction is used to annihilate the stirrer forces and turbulence in the solid metal. In the present study combustion was not considered and the heat source was strongly simplified assuming a radiation boundary condition on top of the metal pad. This assumption can be justified by the fact that the heat transfer in a furnace is strongly dominated by radiation and the main impact of the burner flame is to heat the roof and a radiating furnace atmosphere. As a first approximation it is assumed that the stirrer does not alter the heat transfer conditions at the metal surface besides lowering the surface temperature. The small change of surface temperature of the liquid metal should not have a sensible effect on the roof temperature.

The boundary conditions are summarized in Fig. 10. Compared to previous experiences [7], an increased emissivity of 0.6 was chosen to assure that the heat transfer is not too much limited by the external boundary condition. The stirrer force is an averaged value of the force distribution calculated from supplier information.

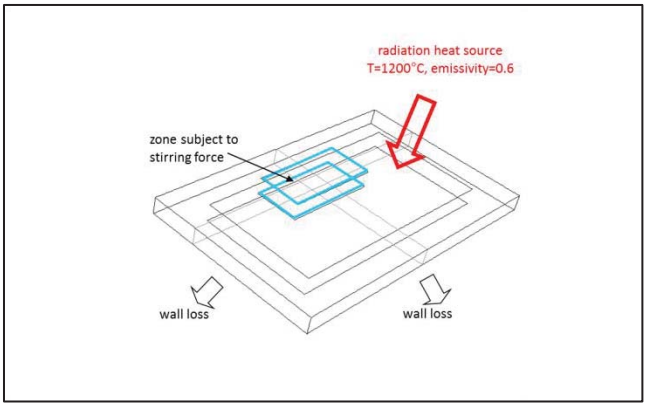

Fig. 10: Model assumptions in the reverberatory furnace study.

The assumptions of the model simplify the real situation drastically: The whole metal charge is allocated inside the furnace as one single solid pad from the very beginning of the cycle. There are no door openings for pushes of cold metal or skimming operations. The calculations are performed fully transient with and without stirring.

Despite the localized stirring force, the generation of instable eddies (as can be seen in the average velocity in Fig. 11) and local surface velocities of up to 1 m/s, the melting of the metal is a smooth process and the liquid solid interface remains a rather flat plane in the simulation (Fig. 11). The evolution of the heat content is recorded and compared with a calculation without stirring. In the calculation without stirring it is difficult to define a realistic end of the melting phase. There is no convection and mixing at all and it takes a very long time, until the last residuals of solid at the bottom disappear, although the metal on top is strongly superheated. In reality, the operators usually perform a mechanical stirring at the end of the melting process to redistribute the superheat and support the melting of remaining solid. Since this is difficult to realize in the model, an alternative was criterion was looked for: The reference time for calculation of the relative improvements was based on the time, when the average temperature of the stirred metal reached the targeted transfer temperature (Fig. 11). At the same time the heat contained in the non-stirred case was determined and both values were compared.

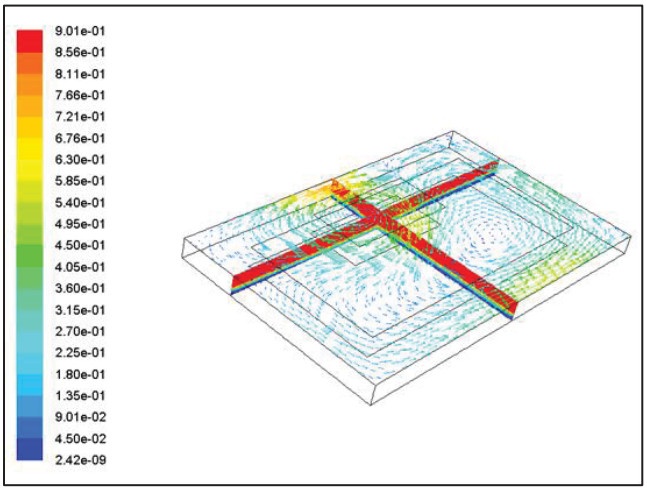

Fig. 11: Surface velocity field and liquid/solid interface after 7000s.

The calculation revealed that for about half of the cycle time there is no liquid at all, which could be stirred. To allow an earlier onset of stirring the original force profile was redistributed to provide a stirring even beyond the physical penetration depth. Even in this optimistic scenario the improvement in total heat pickup was only 8.5%, until the transfer temperature was reached (see Fig. 12).

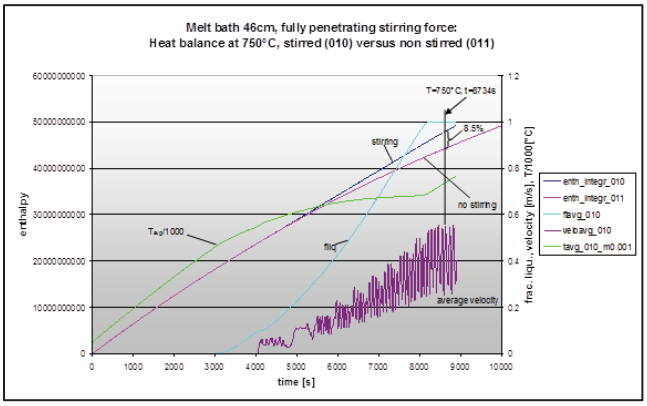

Fig. 12: Comparison of heat pick-up, stirred versus non-stirred.

Cast house experiences

The calculation results could be checked in plant trials after the installation of a new bottom stirrer. It turns out that despite the strong simplifications in the model assumption one major observation is still valid in the real environment: Most of the time there is too few liquid to achieve a visible stirring effect. Fig. 13 shows the last charge of primary ingots 1h after pushing. The push was performed 1h after the start of the cycle, which in total took 3h 30 min until transfer. Most of the material is still solid and blocking the stirrer, which was placed underneath the center of the furnace.

In this state it is a question, which benefit the stirrer should have: The hot furnace atmosphere and the radiating walls transfer heat mainly to solid metal which has a lower temperature and even a higher specific surface than any liquid metal pool. Consequently, the window, when the stirrer generates an effect, is comparatively short.

Fig. 13: Push of primary ingots 1h after charging in a remelting furnace.

The plant tests also revealed several aspects, which need to be considered to come to a fair comparison:

1. Usually, through an upgrade other furnace components beside the stirrer are exchanged or modified. Therefore, comparing production figures before and after the installation does not give an accurate picture of the fraction of improvement, which is exclusively achieved by the stirrer. Comparable figures can only be gained, when all tests with and without stirrer operation are performed after the implementation of the stirrer.
2. Production data of a remelting furnace generally show a considerable scatter from charge to charge. To get a reliable comparison a certain number of heats need to be considered, which should have similar charge weights and consist of similar scrap types. From this and point 1 follows that meaningful validation tests are costly and conflict with the ambition of the plants to run the installation under its optimum conditions, i.e. with stirring.
3. Even if all procedures like pushes, alloying and skimming practice are kept the same and the process only differs in the use of the stirrer, the difficulty remains to measure the target temperature of the melt accurately. Usually this is done by a bath thermocouple which measures a temperature close to the bottom somewhere near the spout. In a stirred furnace the temperature is very homogeneous (dT < 5K), while in an unstirred furnace the temperature difference between top and bottom can be up to 80 K. Depending on the exact position in this temperature field the thermocouple could show a faster or delayed approach to the target temperature compared to a stirred furnace.
4. When analyzing improvement figures of different sources it turns out that it is important to check how relative improvements are calculated. There are different views on how to treat door open times in the evaluation, which lead to different figures.
5. Cycle time reduction and energy consumption are usually linked, although they are sometimes counted as independent benefits. In a first approximation the burners do not feel the presence of the stirrer and run at similar power with or

without stirrer. The main energy savings follow from the reduced runtime of the burners in a faster cycle.

6. Dross figures may interfere with energy consumption. The amount of newly generated oxide inside the dross provides heat, which could reduce the consumption of natural gas. According to thermo-chemical data [8], the heat generated by burning a certain amount of aluminium is theoretically sufficient to melt about 13 times the same amount of solid metal. The measurement of this effect, especially the difference between stirred and non-stirred conditions, is very difficult, since the stirring affects the process by several factors. By stirring the liquid surface could be broken up leading to increased oxidation. On the other hand the increased heat transfer should lower the surface temperature and reduce the oxidation speed. Thirdly, a continuously renewed surface has a lower emissivity. This again reduces the surface temperature, but also the absorption of radiated heat. A reduced surface temperature could increase the metal content of the dross and thereby increase the measured dross weight. Considering all these factors the impact of stirring on dross figures appears to be the most uncertain aspect and might even strongly obscure the fuel balance.
7. Although the stirrer should support the skimming operation by reducing the dross and transporting dross into a preferred skimming area, a bottom stirrer benefits from a powerful skimming machine. Frequently solid metal above the stirrer position blocks and delays the onset of a stirring effect. A strong skimming machine can improve the efficiency of the stirrer by shifting the obstacles.

Improvement potential

Comparing recent experiences on flat hearth furnaces the improvements of energy consumption and melting time are less than 10 percent, while the best references of suppliers are in the order of 15% to 20% [9, 10]. At the moment own measurements during cast house trials and the modeling results appear to be in good agreement, but there are still fields, which need to be clarified or improved and which might explain the gap to the more positive references.

In our model, besides other factors, three major aspects need to be improved:

1. The applied k-epsilon turbulence model of ANSYS Fluent predicts a considerable damping of turbulence at a free surface, which generates a boundary layer, where the effective heat conduction is reduced. This could lower the predicted benefit of a stirrer. Better measurement data, which resolve the thermal profile in the bath are needed to investigate if the existing turbulence treatment is adequate or needs a modified approach.
2. The thermo-physical properties of the liquid surface are assumed to be constant, neglecting any effects of temperature dependency, finite dross layer thickness, entrapped gas bubbles and reactions inside the dross. At least basic oxide growth dynamics seems to be necessary to address the interactions discussed in previous point 6.
3. The heat transfer characteristics through the surface and inside a pile of scrap are very complex. Compared to massive ingots dispersed scrap has a lower effective density, higher specific surface and lower conductivity. During the melting process the metal is compacted and changing its heat transfer properties. Some of these features should be addressed in a future melting model.

In real installations the following areas of improvement can be identified:

1. The usual power ratings of bottom stirrers give only poor information about the stirring effect. It would be easier to compare different systems, if the suppliers could provide information about the stirrer thrust i.e. integrated forces working on standardized metal load in addition to the usual power rating.
2. In present installations the burner control system is usually not modified to account for the stirring device. Since the stirrer is intended to support the heating system, it should be reasonable that the burners take notice of it.
3. A better method than using only one thermocouple would be desired to determine the average temperature of the metal bath for a better comparison of stirred non-stirred charges.

Conclusions

Based on commercially available software packages Hydro Aluminium Rolled Products R&D has developed a modeling toolbox to study the impact of electromagnetic stirrers in reverberatory furnaces. The models appeared to be a valuable tool to enlighten the hidden physics in electro-magnetic stirring and to get an understanding of the basic mechanisms. They helped to adjust expectations, which improvements can be theoretically achieved by stirring, to recent cast house experiences. Despite some good agreement between models and measurements there remain various questions, which need further investigation and might lead to a better exploitation of electro-magnetic stirrers in the future.

References

1. Ludwig Dreyfus, “Induction Stirrer”, *US patent 2513082*, June 27, 1950
2. A. Buchholz, J. Rødseth, “Investigation of heat transfer conditions in a reverberatory melting furnace by numerical modeling”, *TMS Light Metals*, 2011, 1179-1184
3. *ANSYS FLUENT Magnetohydrodynamics (MHD) Module Manual 14.5* (Canonsburg: ANSYS Inc.) 2012, 4
4. Colin J. Smithells, *Metals Reference Book*, 5th edition, (London: Butterworths, 1976), 941, 947
5. Takamichi Iida, Roderick I.L. Guthrie, *The physical properties of liquid metals*, (Oxford: Clarendon Press, 1988), 232
6. V.M. Korovin, ”Forces acting on particles suspended in a current carrying liquid”, *Magnetohydrodynamics*, 1988, 160-165
7. J. Furu et al., “Heating and melting of single al ingots in an aluminium melting furnace”, *TMS Light Metals*, 2010, 679-684
8. *HSC Chemistry 5.1 Chemical Reaction and Equilibrium Software*, (Pori: Outokumpu Research Oy), 2002
9. R. Alchalabi et al., “Furnace operation optimization via enhanced bath circulation”, *TMS Light Metals*, 2002, 739-746
10. R. Stal et al., “Establishing operational parameters of al-ems using numerical simulations to promote energy efficiency during final heating in aluminium furnaces”, *TMS Light Metals*, 2010, 657-661